ELSEVIER

Microelectronic Engineering 65 (2003) 87–101

MICROELECTRONIC ENGINEERING

www.elsevier.com/locate/mee

Study on linearity of a micromachined convective accelerometer

X.B. Luo[a], Z.X. Li[a,*], Z.Y. Guo (Professor)[a], Y.J. Yang[b]

[a]*Department of Engineering Mechanics, Tsinghua University, Beijing 100084, China*
[b]*Hebei Semiconductor Research Institute, Shijiazhuang 050051, China*

Received 6 March 2001; accepted 19 March 2002

Abstract

The linearity of a micromachined convective accelerometer without solid proof mass is numerically and experimentally studied in this paper. The accelerometer consists of a micro heater and two temperature sensors which measure the gas temperature difference between two symmetrical positions on both sides of the micro heater. The temperature difference is caused by free convection due to acceleration. The simulation results show that the output of the convective accelerometer is linear with the Grashof number only when the Grashof number is smaller than 10^3 and larger than 10^{-2}. It will be favorable for achieving good linearity and high sensitivity synchronously as the non-dimensional sensor position, defined by the ratio of the distance from the heater to the half cavity length, is around 0.3. Design considerations are given based on the simulation analysis, a micromachined convective accelerometer is manufactured by bulk-silicon fabrication, the test results demonstrate that it has good linearity and high sensitivity.

Keywords: Micromachined convective accelerometer; Linearity; Grashof number

1. Introduction

Demands for low-cost and high-performance accelerometers have been increasing in many fields including the automobile industry, navigation systems, the military industry, robotics systems, consumer electronics and toys [1]. Many efforts have been made in developing micromachined accelerometers in recent years to meet the cost and performance requirements [2–7].

So far, the common designs of micromachined accelerometers involve solid proof mass, which is allowed to move under accelerating conditions. The existence of the proof mass brings some disadvantages to the accelerometers. Firstly, the ability to resist shock declines, the overload range can not be wide. Secondly, the fabrication is complex and not suitable to IC techniques, consequently the

*Corresponding author. Tel.: +86-10-6277-2919; fax: +86-10-6278-1610.
E-mail address: lizhx@tsinghua.edu.cn (Z.X. Li).

0167-9317/03/$ – see front matter
PII: S0167-9317(02)00731-1

size can not be very small and the start-up cost can not be reduced. Thirdly, the motion sensor of solid mass proof suffers from some problems [7], for example capacitive sensing, the most common sensing method, suffers from the electromagnetic interference and the influence of parasitic electrostatic force.

Recently, a novel concept and device structure for acceleration measuring were developed by Dao et al. [8], operation of the accelerometer is based on free convection of a tiny hot air bubble in an enclosed chamber. It does not require solid proof mass and is compact, lightweight, inexpensive to manufacture and sensitive to small acceleration. Leung et al. [9] reported the implementation of the device structure by bulk silicon fabrication, the test for the device under natural gravity demonstrates that its sensitivity can reach 0.6 mg. Milanovic et al. [10] fabricated two kinds of the convective accelerometers, thermopile and thermistor types in standard IC techniques. Their accelerometers exhibit some significant advantages such as low cost, miniaturization, integration and good frequency response.

Linearity is an important index for accelerometers, good linearity will offer much convenience to applications. Since the convective accelerometer is convection-based, the heat and mass transfer in the device are complicated. The following problems will come forth before us, whether the output of the convective accelerometer can be linear with acceleration/Grashof number or not, under what conditions can a good linearity be obtained?

In this paper, numerical simulations are conducted for studying the factors affecting the linearity of convective accelerometer and optimizing the working parameters. According to the analyses, a kind of micromachined convective accelerometer is fabricated, the experimental results show that it has good linearity and high sensitivity.

2. Device structure and basic principles

Fig. 1 shows the device structure of a micromachined convective accelerometer. It includes an electric heater and two temperature sensors mounted within a sealed enclosure containing a kind of

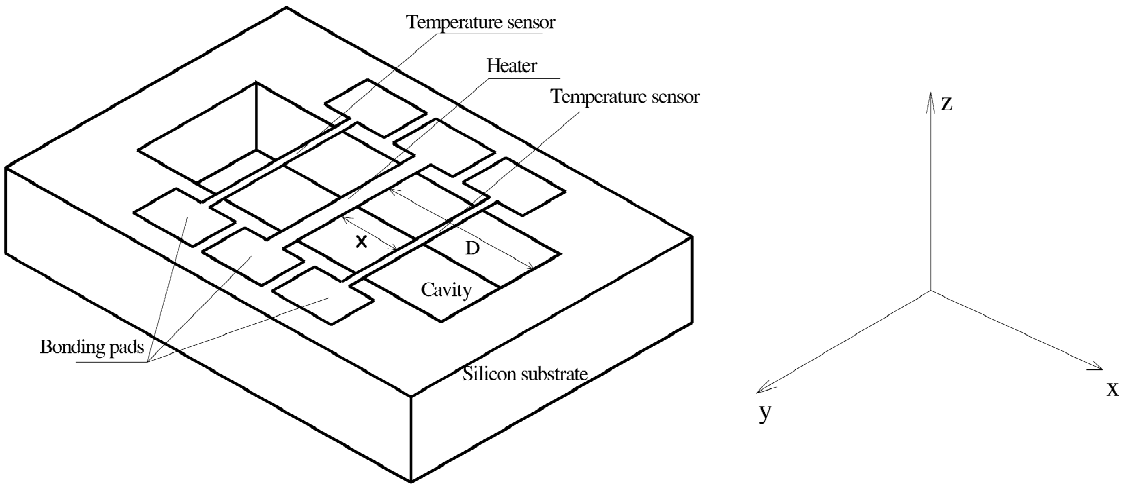

Fig. 1. Device structure of a micromachined convective accelerometer.

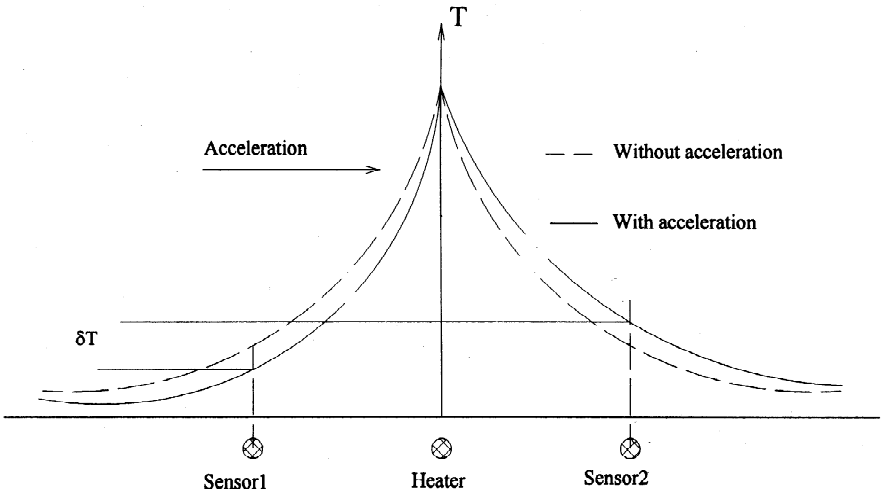

Fig. 2. The symmetrical temperature distribution generated by the central heater is disturbed by applied acceleration.

gas. The sealed enclosure aims to prevent environmental air flow from disturbing the device's operation. The temperature sensors are positioned symmetrically on both sides of the microheater. The microheater is used to heat the gas and therefore to create a free convection when acceleration is applied to the gas. The heater temperature and gas temperature distributions along the X axis are illustrated in Fig. 2. In the case of no acceleration or the acceleration normal to the X axis of the accelerometer, the flow pattern and gas temperature distribution are symmetrical as the dash lines show due to the symmetric locations of two temperature sensors. As a result, no temperature difference exists between two temperature sensors no matter how high the heater temperature is. As long as the acceleration at X axis appears, the free convection along X axis is produced or the gravity induced convection is skewed. This must lead to the asymmetric distributions of gas temperature shown by the solid lines in Fig. 2. Consequently, the temperature difference between two sensor positions becomes non-zero. Apparently, the temperature difference between two sensors increases with increasing the acceleration at the X axis. By measuring the temperature difference, the acceleration information can be acquired.

3. Linearity analysis

For the linearity of a convective accelerometer, as illustrated in the above section, it requires that the voltage engendered between two temperature sensors is linear with the exerted acceleration. To actualize this, it is necessary to assure the following two points for the device. Firstly, the temperature difference between the two temperature sensors linearly relates with acceleration. Secondly, the output voltage is linear with the temperature difference. The former is the key factor to obtain good linearity for the convective accelerometer, which will be mainly focused on in this paper. As for the latter, it is mainly decided by the material property of the temperature sensor. Linear dependence of resistance on temperature of the material is appreciated for the linearity. Usually, the temperature sensors are made of polysilicon in micromachined process. Polysilicon produced in different processes is of different variances of resistance with temperature, in order to make the output of the convective accelerometer

being linear with acceleration, a suitable fabrication process should be chosen so as to provide a linear relation between sensor temperature and its resistance. In following analysis, we will focus on the relation of the temperature difference of two sensors with acceleration.

3.1. Governing equations and numerical simulation

Since the dimensions of the micromachined convective accelerometer and the gas velocity are small, the gas flow is usually laminar. The free convection is caused by the body force due to acceleration and the spatial density variation resulted from the spatial temperature change in the enclosure. The governing equations are as follows:

Equation of continuity:

$$\nabla \cdot u = 0 \tag{1}$$

Equation of momentum:

$$\rho u \cdot \nabla u = -\nabla p + \mu \nabla^2 u + \rho a \tag{2}$$

Equation of energy:

$$\rho c_p u \cdot \nabla T = k \nabla^2 T \tag{3}$$

Equation of state:

$$\rho = \frac{p}{RT} \tag{4}$$

where u, ρ, p, a, $T$are velocity, density, pressure, acceleration and temperature respectively, μ, c_p, k are dynamical viscosity, specific heat and thermal conductivity respectively, R denotes the ideal gas constant.

Obviously, it is very difficult to have analytical solution for above-mentioned equations, thus we conduct numerical simulation. The commercial code named STAR-CD is adopted for the simulation. In the computations, μ, c_p, k are given the constant values at the average temperature of the heater and environment.

For the device shown in Fig. 1, because the ratio of the lengths of heater and temperature sensors to their widths and heights is very large, a two dimensional model can be adopted. Fig. 3 shows the convective accelerometer model we simulate. L denotes the heater width, D denotes half of the cavity length at the bottom part, d represents the cavity depth, x represents the distance between sensor and heater. For simplicity, both heater surface and cavity wall are regarded as isothermal. In the computations, different grid sizes are adopted, fine grid is adopted in the region near heater, direction of acceleration a is towards the left.

The following numerical simulations and analyses are made starting from a realized prototypes having such characteristics: the temperature of heater surface is 973 K, the cavity size is 960×100 μm, the gas media is air. The simulation results of flow and temperature distributions for one case that the acceleration at sensitive axis is 10 g ($g = 9.81\ \mathrm{m/s^2}$) are shown in Fig. 4. Fig. 4a shows the

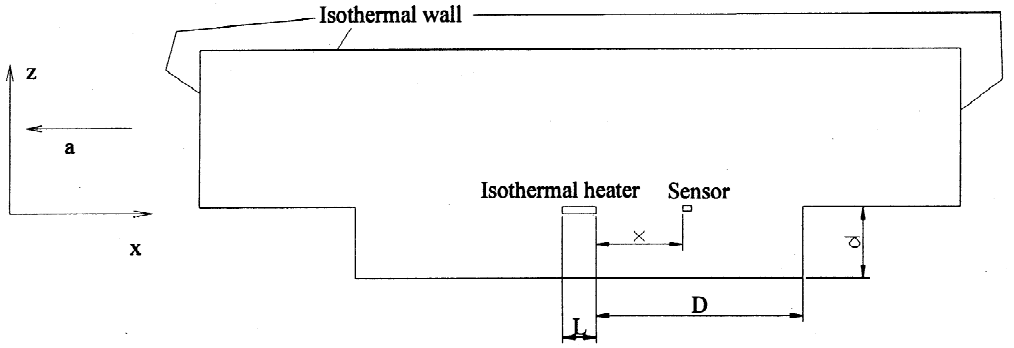

Fig. 3. Schematic of simulated convective accelerometer.

velocity distribution in the convective accelerometer. It can be seen that the flow direction of the fluid is towards left near the heater when subjected to acceleration, asymmetrical flow forms in the cavity. Fig. 4b demonstrates the temperature distribution in the convective accelerometer. It is obvious from Fig. 4b that the isothermal lines in the cavity are not symmetrical to the heater. The temperature of the fluid in the left side of the heater is higher than that in the right side because of the asymmetrical flow in the cavity.

3.2. Results and discussion

Dimensional analysis on the governing Eqs. (1), (2) and (3) shows that two dimensionless parameters, the Grashof number Gr, the Prandtl number Pr, govern the free convection [11]:

$$\mathrm{Gr} = \frac{a\beta\Delta T L^3}{\upsilon^2} \tag{5}$$

$$\mathrm{Pr} = \frac{\upsilon}{\alpha} \tag{6}$$

where β, υ, α are bulk expansion coefficient, kinetic viscosity, and thermal diffusivity, respectively, ΔT is the temperature difference between heater and cavity wall.

It is obvious from Eq. (6) that the Prandtl number is decided by the working gas filled in the convective accelerometer. Thus for an accelerometer that gas media is given, the flow and heat transfer in it are determined only by the Grashof number, which implies that the temperature difference between the two sensors is also decided by the Grashof number. In fact, the convective accelerometer is given in a certain application, the parameters in the definition of Grashof number such as β, ΔT, L, υ will be given, thereby the Grashof number is just proportional to acceleration based on Eq. (5). So, the dependence of the temperature difference on the Grashof number represents the relation of the temperature difference with acceleration, this will be the base of the following linearity discussion. Fig. 5 depicts the dependence of the temperature difference on the Grashof number.

In Fig. 5, both abscissa and ordinate adopt logarithmic coordinates, the ordinate δT represents the temperature difference between two sensors. It can be seen from Fig. 5 that for Grashof number, in

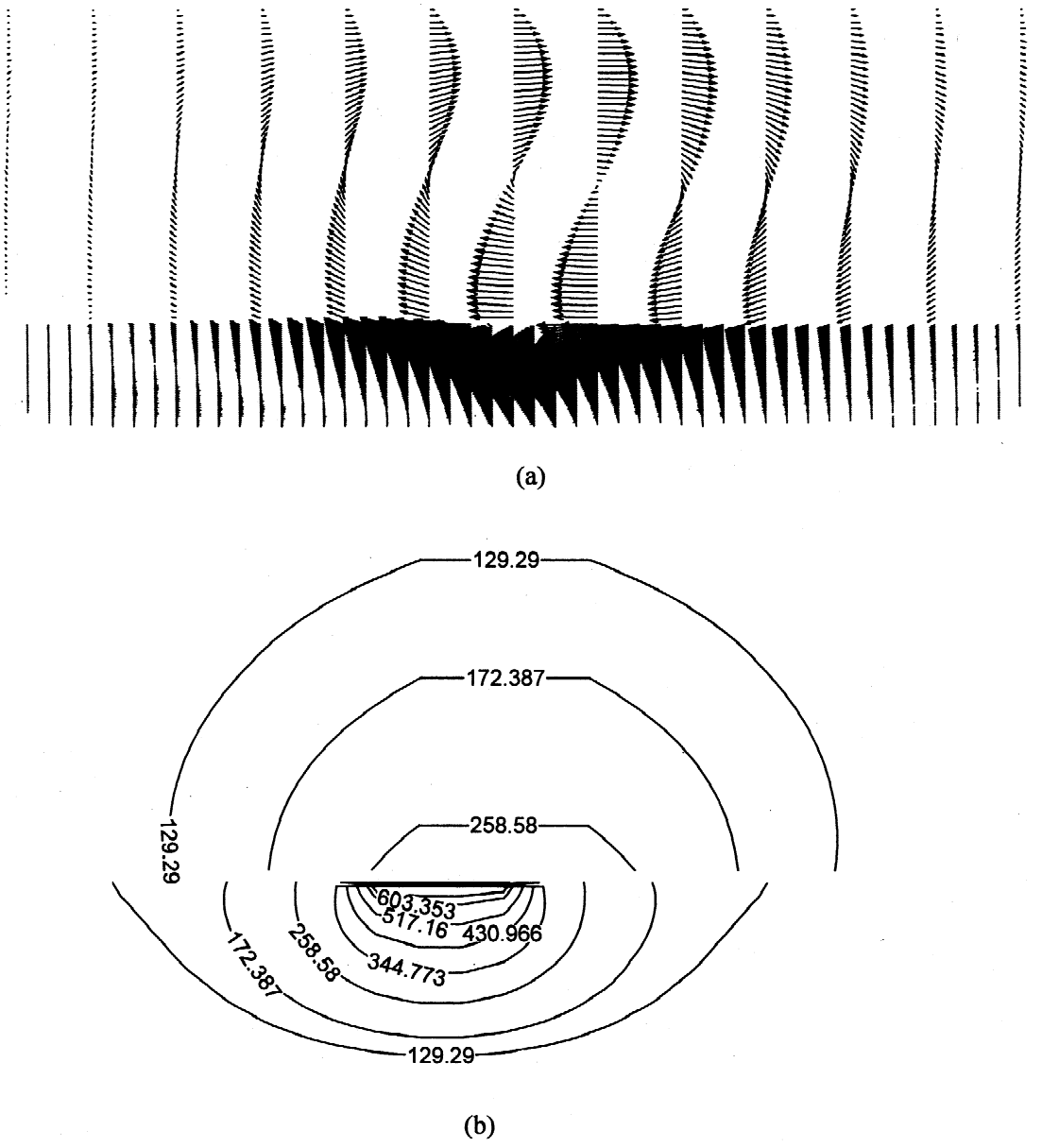

Fig. 4. Simulation results at heater temperature of 973 K (a) velocity distribution (b) temperature distribution.

the range of larger than 10^{-2} and smaller than 10^{3}, the temperature difference is almost linear with Grashof number. That is to say, in the above range for Gr, the output of the convective accelerometer is linear with acceleration. Why does the linear relation exist in this Gr region? It can be explained as follows. There are three forces, inertial force, viscous force and buoyancy force, which govern the natural convection. For the natural convection with large Grashof number resulted from large scale,

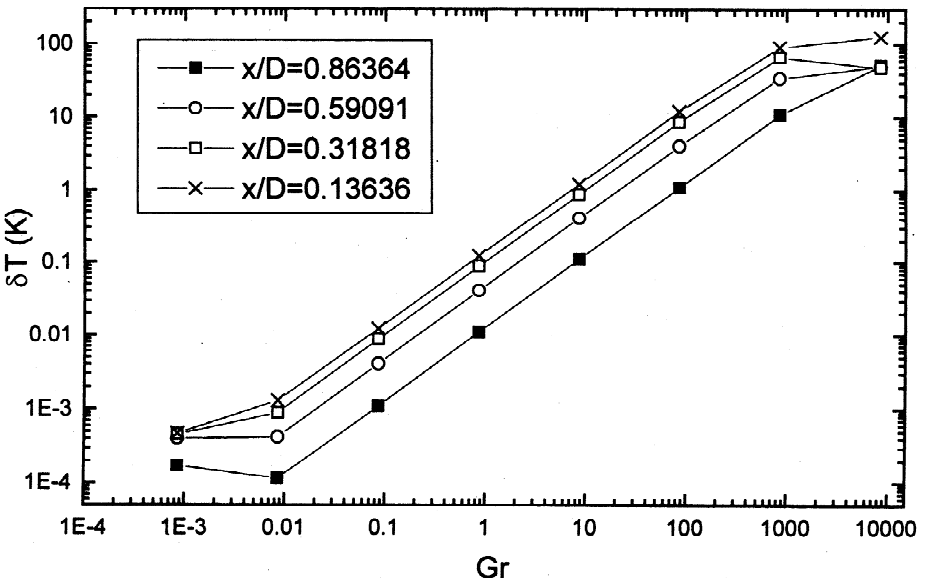

Fig. 5. The temperature difference versus Gr.

large temperature or large acceleration, the inertial force term is not too small to be neglected compared to viscous force, thus the governing equations show non-linearity characteristics, consequently, the flow and heat transfer in the accelerometer exhibit non-linearity. For the natural convection with very small Grashof number, heat conduction in the convective accelerometer overwhelmingly prevails over the convection, thereby the non-linearity in small Gr condition may be contributed to the increasing influence of the heat conduction where the inertial force is very small compared to viscous force. Only in the range of Gr larger than 10^{-2} and smaller than 10^{3}, the convective accelerometer exhibits a performance of output linear with acceleration. The reason is that the natural convection in the accelerometer is governed by both viscous force and buoyancy force, the inside heat conduction is not too strong compared to the natural convection.

Because the temperature difference is linear with the Grashof number, obviously, larger Grashof number will create larger temperature difference, that is to say, the accelerometer design of large Grashof number will result in high sensitivity for a given accelerometer.

The effect of sensor position on the linearity of the convective accelerometer is also simulated, the result is illustrated in Fig. 6. The abscissa x/D denotes the non-dimensional position of the temperature sensor, the ordinate denotes the linearity error, which is defined as the real numerical results divided by the value obtained from the fitting line. It is noted from Fig. 6 that the linearity error is smallest when x/D ranges from 0.3 to 0.7, where it is around 0.05%. When the sensor is positioned at other position, it can increases to 0.5%, so suitable sensor position will be advantageous to the linearity improvement. The dependence of the sensitivity on the sensor position at different Gr is shown in Fig. 7. It is seen that the sensor position for high sensitivity has an optimum place, which is around $x/D = 0.2$. When apart from this position, the sensitivity will decline. Based on the above discussions, the sensor position for good linearity and high sensitivity synchronously is around

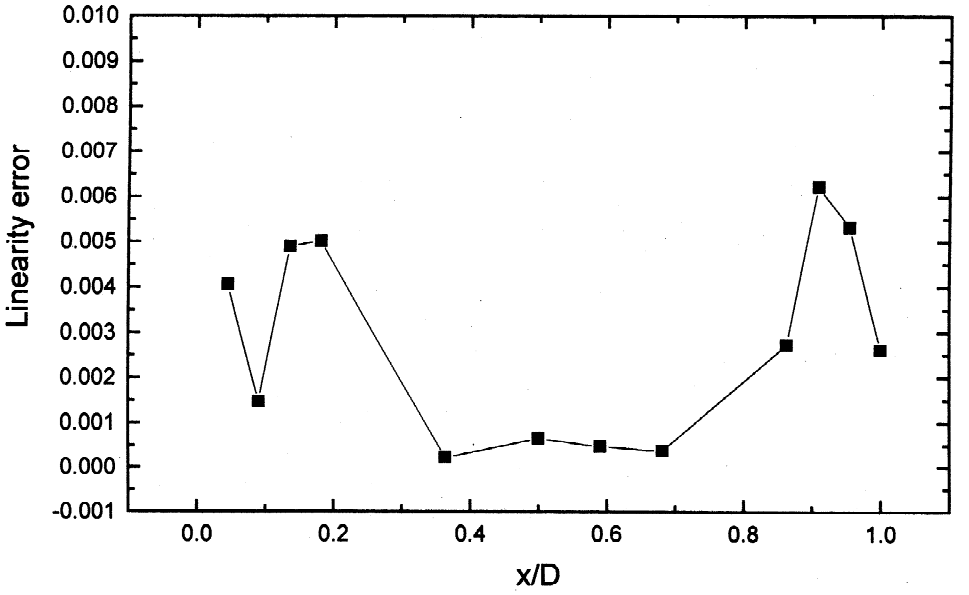

Fig. 6. The linearity error versus the sensor position.

$x/D=0.3$. It is also noted from Fig. 7 that the sensitivity (temperature difference) increases with Grashof number increase.

To sum up, it is necessary to guarantee the Grashof number in the range of $10^{-2}\sim10^{3}$ to achieve good linearity, the Grashof number should be designed as large value for high sensitivity providing that good linearity has been achieved. The sensor position, $x/D=0.3$, will be favorable for the

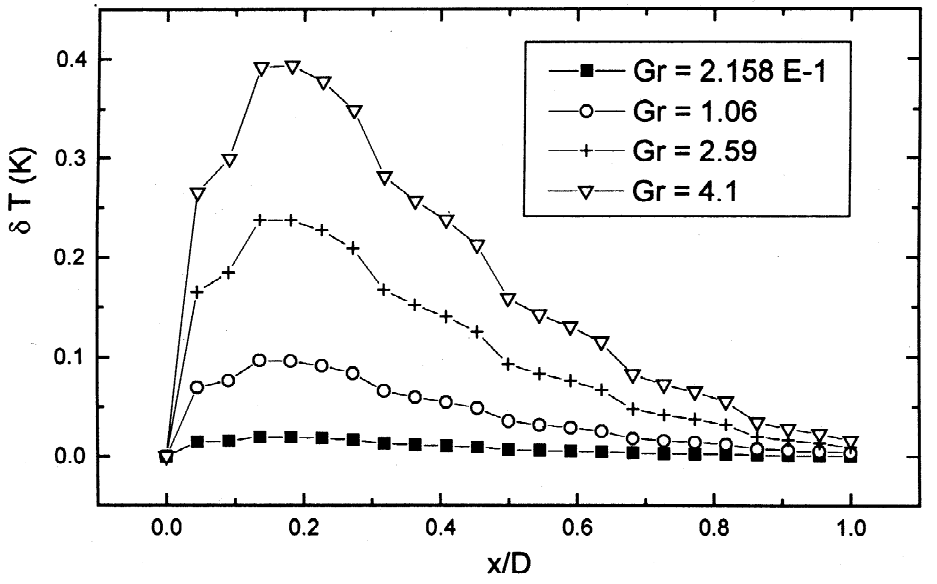

Fig. 7. The variation of temperature difference with sensor position.

convective accelerometer design to obtain good linearity and high sensitivity synchronously in applications.

4. The design consideration

Based on Eq. (5) and the foregoing analysis, to achieve good linearity and high sensitivity, the temperature difference ΔT, heater width L, the filled gas, sensor position x/D should be considered in design. In addition, compared with the heater width, if the cavity size is not large enough to be regarded as infinite space, it should also be taken into account because of the boundary suppressing action on fluid flow.

It is obvious from Eq. (5) that Grashof number Gr increases with increasing ΔT (in other words, increasing the heating power), heater width L and bulk expansion coefficient β of the gas filled in the accelerometer and decreases with increasing the kinetic viscosity υ. Especially, increasing the heater width L will lead to a significant increment of Gr owing to the cubic relation of Gr with L. Therefore, to assure the accelerometer obtaining good linearity, the above parameters, especially$L$ should be carefully chosen. At the same time, to increase the sensitivity, we should make the temperature of the heater surface high enough, the heater width is designed as a large size. As for cavity design, it should be designed to be large to reduce the boundary suppressing action. For sensor position, as analyzed in the preceding discussions, the best place is near $x/D = 0.3$.

5. Fabrication

The device fabrication sequence is illustrated in Fig. 8. Starting with a $\langle 100 \rangle$ silicon substrate, a layer of silicon dioxide is formed using wet thermal oxidation, then a uniform layer of polysilicon is deposited in low-pressure chemical vapor deposition (LPCVD) reactor and another layer of silicon dioxide is grown on it (Fig. 8a). The top oxide and polysilicon layers are patterned to engender heater, temperature sensor and polysilicon contact. After patterning, the polysilicon sidewalls are exposed (Fig. 8b). Then an oxide layer is produced on the polysilicon sidewalls by another oxidation step, which protects polysilicon from anisotropic etching using ethylene diamine–pyrocatechol (EDP). On the oxide layer, the bonding pad and cavity windows are opened (Fig. 8c). A boron layer is then used to dope the silicon regions for making electrical connections to the heater and sensors, afterward by the patterned photolithography, a layer of Ti/Pt/Au metal is sputtered onto the top surface (Fig. 8d). When the metal is stripped, bonding pads and the cavity windows form (Fig. 8e). Finally, the wafer is wet-etched in EDP until the cavity's creation (Fig. 8f). Fig. 9 is a scanning electron microscopy (SEM) photograph of the device that is sealed in an enclosure.

6. Experiments

One micromachined convective accelerometer is fabricated according to the above process. The heater width is 80 μm, the height is 2 μm, the cavity size is 3000 (length) × 2000 (width) × 250 (depth) μm, the sensor position is near $x/D = 0.34$.

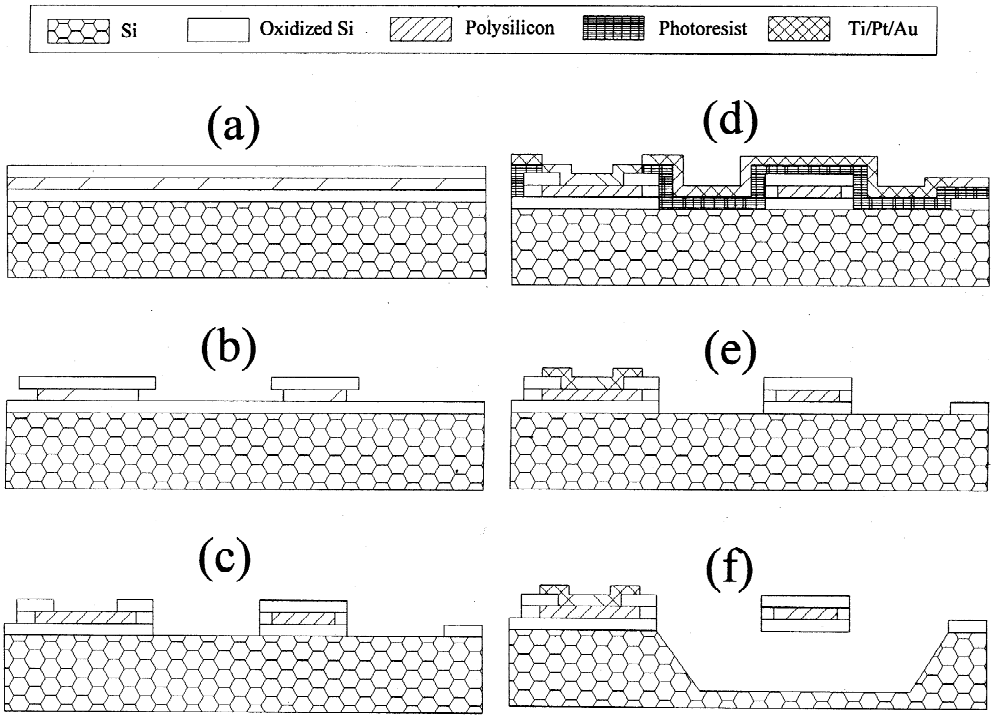

Fig. 8. Device fabrication sequence.

It is measured under two kinds of application conditions. Firstly, it is tested from $-g$ to g under gravitation by rotating of the sensitivity axis with respect to the earth gravitational field. Fig. 10 illustrates the linearity of the accelerometer under gravitation. It shows a very good fit with the

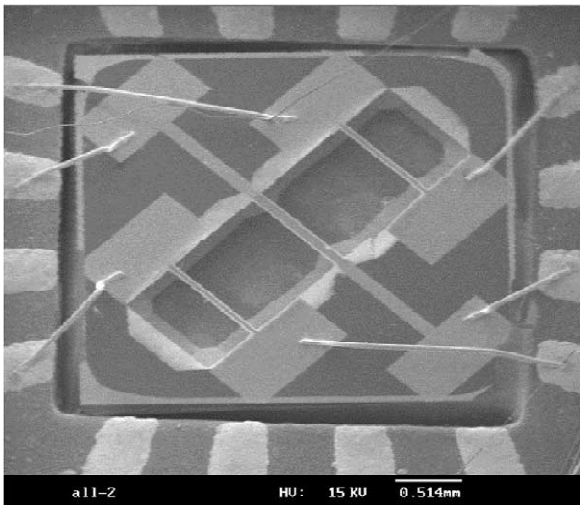

Fig. 9. SEM photograph of the device sealed in a enclosure.

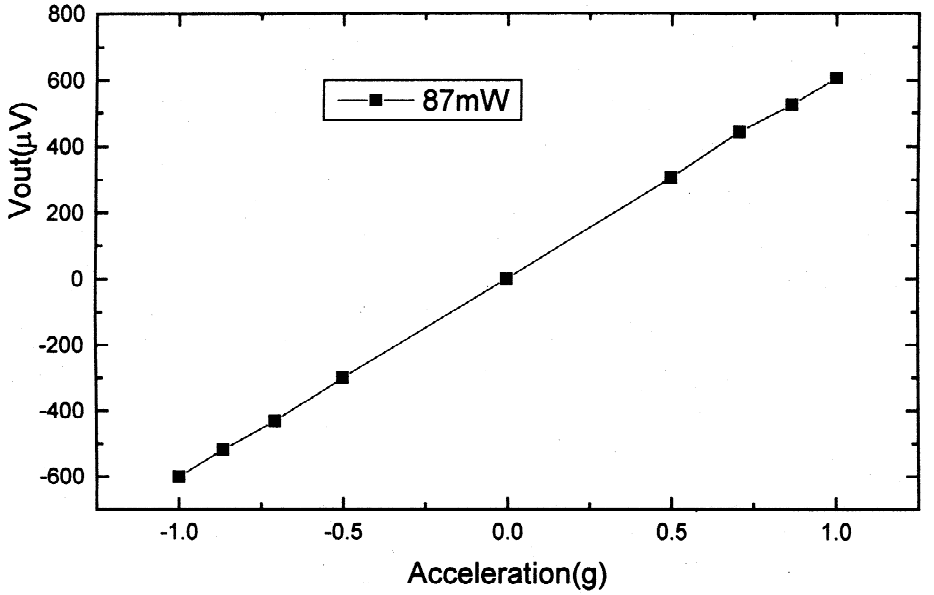

Fig. 10. The linearity of the optimized accelerometer at 87 mW under gravitation.

expected linear trend. The linearity error is smaller than. For a comparison, the non-linear coefficient of the accelerometer in Ref. [9] under gravitation is obviously larger than 1% at the 1 *g* point and that of the device in Ref. [9] is 0.5%.

The device is also measured on a vibration shaker with acceleration range from 0 to 20 *g* and

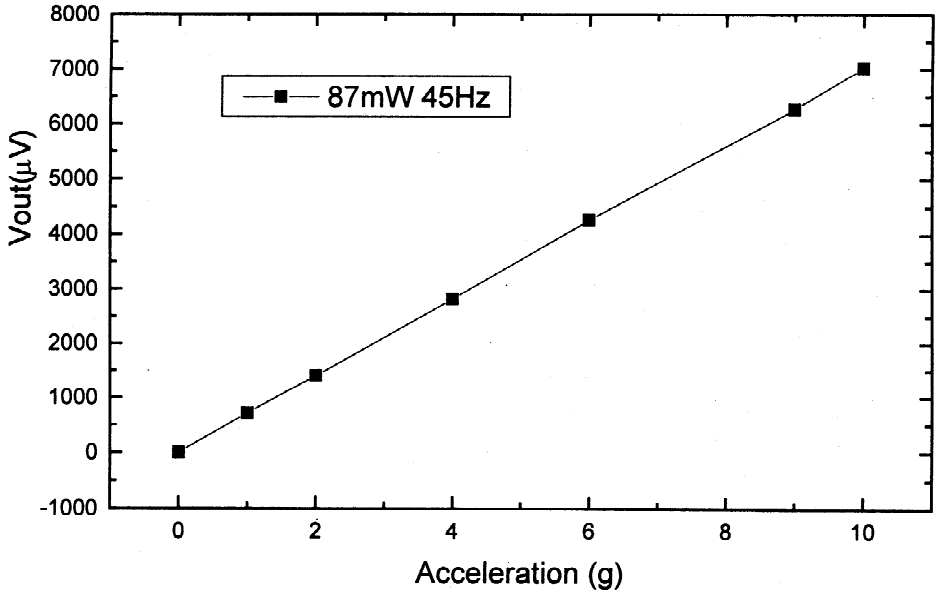

Fig. 11. Measured performance of the accelerometer at 87 mW from 0 to 10 *g*.

frequency from 0 to 200 Hz. In our experiments, we find that when the acceleration range exceeds 10 *g*, good performance especially for good linearity can not be achieved. Fig. 11 shows that the device has good linearity in the range from 0 to 10 *g* at 45 Hz. The linearity error is larger than that measured under gravitation, which reaches 2%. It is noted from Fig. 11 that the sensitivity of the optimized accelerometer for operating power of 87 mW is 600 μV/g, where the sensitivity does not include the circuit amplification. For a comparison, the sensitivity of the accelerometer in Ref. [10] is 146 μV/g for an operating power of 430 mW, the linearity error in acceleration range from 0 to 7 *g* is 2%. Owing to the absence of relative comparable data, here the comparison with that in Ref. [9] can not be carried out.

The frequency response of the device is shown in Fig. 12. It is noted that the frequency response is flat up to about 75 Hz, where the sensitivity decreases substantially. The response frequency is larger than that in Ref. [9], in which it is 20 Hz. However, compared with the response frequency numbered 300 Hz in Ref. [10], it is much smaller. The main reason for this may contributes to the fabrication method and the accelerometer size. In our present work, same as that in Ref. [9], customary bulk-silicon fabrication is adopted, the accelerometer size including cavity size are larger than that in Ref. [10], in which standard integrated circuits technology was employed. Based on foregoing optimization analysis, the frequency characteristics of the present accelerometer can not be satisfactory as that in Ref. [10].

The noise test is also performed. The 25-Hz output noise at operating power of 87 mW is 0.6 $\mu V/\sqrt{Hz}$, so the noise equivalent acceleration (NEA) of the present convective accelerometer at 25 Hz is approximately 1 $mg/\sqrt{Hz}$.

An investigation into the dependence of the sensitivity on the heating power is also conducted in the test under gravitation. Fig. 13 shows that the sensitivity of the accelerometer is nearly linear with the heating power, it proves that increasing heating power can increase sensitivity.

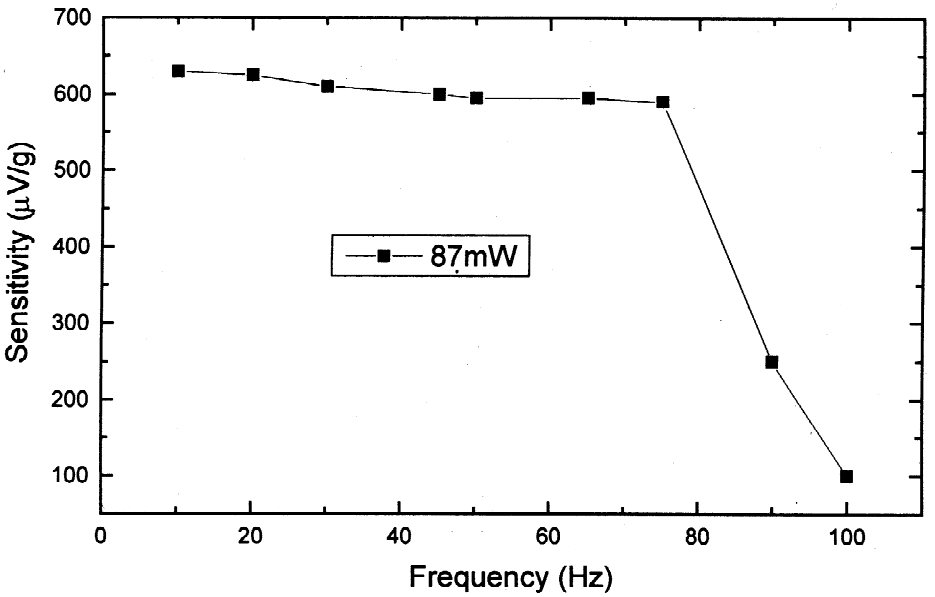

Fig. 12. Measured frequency responses.

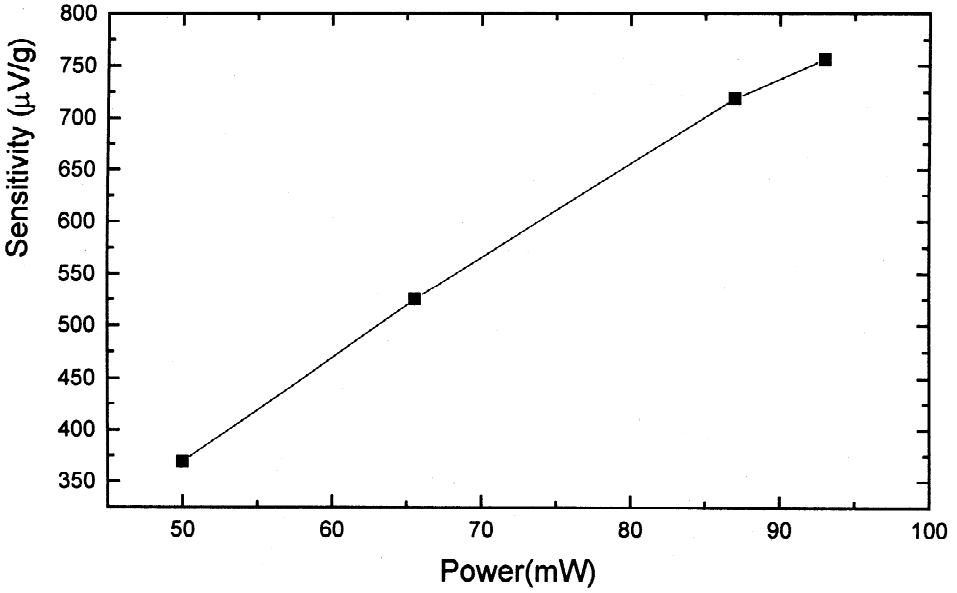

Fig. 13. The variation of sensitivity with heater power.

The variation of NEA with the heating power at 25 Hz is demonstrated in Fig. 14. It is noted that NEA of the convective accelerometer decreases with heating power increasing, which can be explained by the fact that when the heating power increases, the sensitivity increases linearly,

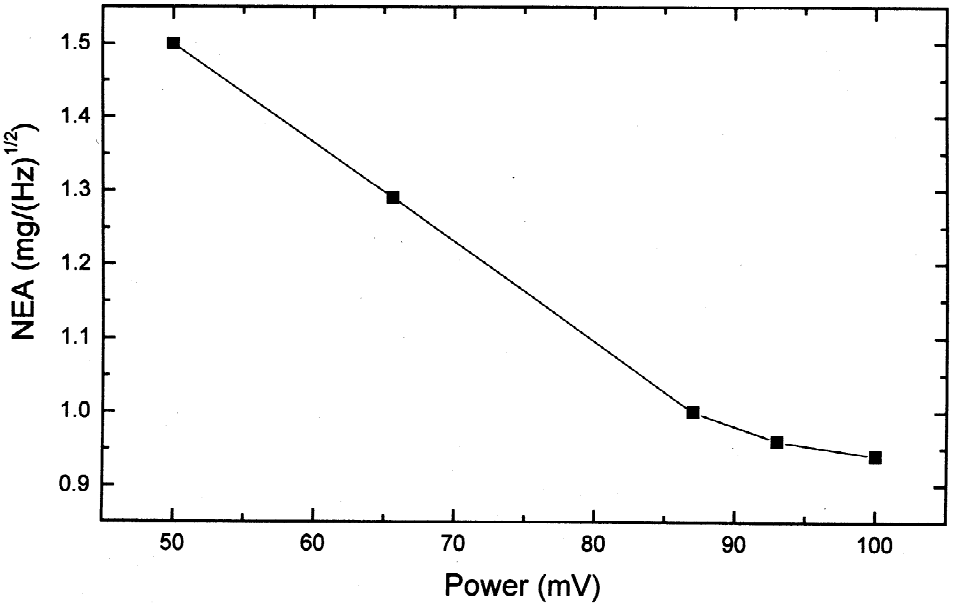

Fig. 14. The variation of resolution with the heating power.

however, the noise just increases slightly. So, higher heating power will be favorable for gaining better resolution.

7. Conclusions

In this paper, linearity of a convective accelerometer is numerically studied. Simulation results show that the output of the convective accelerometer is linear with the Grashof number when the range of Gr is smaller than 10^3 and larger than 10^{-2}. The temperature sensor position ranging from 0.2 to 0.7D will assure the accelerometer having a good linearity. By considering linearity and sensitivity, the temperature sensor positioned at around $x/D=0.3$ will be favorable for achieving a good linearity and a high sensitivity synchronously. The heater surface temperature, heat width should be carefully chosen in the design. The cavity size should be designed to be large so as to obtain high sensitivity. A micromachined convective accelerometer is fabricated and tested. The experimental results demonstrate that the linearity error of the accelerometer is smaller than 0.35% under natural gravity and smaller than 2% in the case of acceleration ranging from 0 to 10 g. A sensitivity of 600 μV/g is measured for operating power of 87 mW. The response frequency is about 75 Hz and the corresponding NEA is approximately 1 mg/$\sqrt{\text{Hz}}$ at 25 Hz. Both linearity and sensitivity of the accelerometer are better than those reported in the literature.

Acknowledgements

This work was supported by the National Natural Science Foundation of China (grant No. 59995550-2).

References

[1] C. Song, M. Shinn, Commercial vision of silicon-based inertial sensors, Sensors Actuators A 66 (1998) 231–266.
[2] N. Yazdi, F. Ayazi, K. Najafi, Micromachined inertial sensors, Proc. IEEE 86 (1998) 1640–1659.
[3] K.H. Kim, J.S. Ko, Y.H. Cho, K. Lee, B.M. Kwak, A skew–symmetric cantilever accelerometer for automotive airbag applications, Sensors Actuators A 50 (1995) 121–126.
[4] Y. Nemirovsky, A. Nemirovsky, P. Muralt, N. Setter, Design of a novel thin film piezoelectric accelerometer, Sensors Actuators A 56 (1996) 239–249.
[5] R.L. Kubena, G.M. Atkinson, W.P. Robinson, F.P. Stratton, A new miniaturized surface micromachined tunneling accelerometer, IEEE Electron Device Lett. 17 (1996) 306–308.
[6] U.A. Dauderstadt, P.H.S. de vries, R. Hiratsuka, P.M. Sarro, Silicon accelerometer based on thermopiles, Sensors Actuators A 46–47 (1995) 201–204.
[7] O. Bochobza-Degani, D.J. Seter, E. Socher, Y. Nemirovsky, Comparative study of novel micromachined accelerometers employing MIDOS, Sensors Actuators A 80 (2000) 91–99.
[8] R. Dao, D.E. Morgan, H.H. Kries, D.M. Bachelder, Convective accelerometer and inclinometer, US Pat. 5 581 034, 1996.

[9] A.M. Leung, J. Jones, E. Czyzewska, J. Chen, M. Pascal, Micromachined accelerometer with no proof mass, in: Technical Digest of International Electron Device Meeting (IEDM 97), 1997, pp. 899–902.
[10] V. Milanovic, E. Bowen, M.E. Zaghloul et al., Micromachined convective accelerometers in standard integrated circuits technology, Appl. Phys. Lett. 76 (4) (2000) 508–510.
[11] P.H. Oosthuizen, D. Naylor, Introduction To Convective Heat Transfer Analysis, WCB/McGraw-Hill, New York, 1999.